

Global Sediment Thickness Dataset

updated for the Australian-Antarctic Southern Ocean

Joanne Whittaker^{1*}, Alexey Goncharov², Simon Williams³, R. Dietmar Müller³,
German Leitchenkov⁴

Corresponding author: jo.whittaker@utas.edu.au

Key Points

- Global minimum sediment thickness compilation updated for Australia
Antarctica
- Sediment thicknesses computed from seismic reflection and refraction data
- Sediment thicknesses up to 9 km thicker than previously estimated

Abstract

We present a new, 5-minute sediment thickness grid for the Australian-Antarctic region (60°–155°E, 30°–70°S). New seismic reflection and refraction data have been used to add detail to the conjugate Australian and Antarctic margins and intervening ocean floor where regional sediment thickness patterns were poorly known previously. On the margins, sediment thickness estimates were computed from velocity-depth functions from sonobuoy/refraction velocity solutions ground-truthed against seismic reflection data. For the Southeast Indian Ridge

This article has been accepted for publication and undergone full peer review but has not been through the copyediting, typesetting, pagination and proofreading process which may lead to differences between this version and the Version of Record. Please cite this article as doi: 10.1002/ggge.20181

abyssal plains, sediment thickness contours from Geli et al. (2007) were used.

The new regional minimum sediment thickness grid was combined with the global NGDC sediment grid (Divins, 2004) to create an updated global grid. Even using the minimum estimates, sediment accumulations on the extended Australian and Antarctic continental margins are 2 km thicker across large regions and up to 9 km thicker in the Ceduna Basin compared to the global NGDC compilation of sediment thickness data.

Introduction

The NGDC sediment thickness map and dataset (Divins, 2004) provides minimum sediment thickness estimates for the world's margins and oceans, and is a well-used resource. It is utilized as an input for tackling a variety of scientific problems, including computing the depth-age relationship of the ocean floor, understanding the origin of oceanic depth anomalies, restoring continental margin extension and deriving continental fit reconstructions, and understanding the thermal structure and heatflow of continental margins.

However, the sediment thickness estimates included in this dataset for the Southeast Indian Ridge region and conjugate southern Australian and Wilkes Land, Antarctic margins are unreliable due to an absence of quality publically available data. This situation has led to the exclusion of the Southeast Indian Ridge and conjugate Australian-Antarctic margins areas from global analyses, for example the calculation of lithospheric thinning along continental margins by Crosby et al. (2011). Here we use seismic reflection and refraction data to create grids of minimum and maximum estimated sediment thickness for the Southeast Indian Ridge region and use the minimum estimate to update the global NGDC

compilation. The updated sediment thickness grid is available from the National Oceanic and Atmosphere Administration's (NOAA) online National Geophysical Data Center at <http://ngdc.noaa.gov/mgg/sedthick/>.

Methods and Results

We compute new, regional 5-minute resolution sediment thickness grids using seismic reflection and refraction derived sediment thicknesses for the southern Australian and conjugate Antarctic Wilkes Land margins, merged with sediment thickness data from Géli et al. (2007) for the intervening abyssal plains. Values from the NGDC global sediment thickness grid (Divins, 2004) were used for areas not covered by the other data sets.

Estimating Australian-Antarctic conjugate margin sediment thicknesses

To constrain sediment thickness along the Southern Australian and conjugate Wilkes Land, Antarctic margins we used total sediment thickness (depth from seafloor to acoustic basement interpreted to represent the top of igneous crust) interpreted in reflection data in two-way time (Stagg et al., 2005; Whittaker et al., 2010) and the co-located velocity solutions from refraction and sonobuoy data (Figure 1).

Seismic reflection data off the East Antarctic margin (~36°E–152°E) were collected by Geoscience Australia during the Antarctic summers of 2000/01 and 2001/02. This major deep water geophysical data set included high-quality deeply penetrating multichannel seismic data with coincident gravity, magnetic and bathymetry data (Stagg et al., 2005).

The reflection seismic data along the southern and southwestern Australian continental margins include 55,900-line km of variable quality data. These seismic data range from coarse grids with line spacing of 10–50 km to regional seismic surveys (Bradshaw et al., 2003; Sayers et al., 2001).

The sonobuoy/refraction data are compiled from surveys extending from the 1970's to 2009. The data include mostly non-reversed recordings of marine survey reflection shots by the sonobuoys deployed during these surveys and recording data up to 20 km offsets, thus allowing velocity characterization down to the bottom of sediments. These velocity solutions are summarized in Sayers et al. (2001) for the Australian Southern Margin and in Stagg et al. (2005) for the Antarctic Margin. In addition, on the Antarctic Margin we also use reversed sonobuoy recordings from the Russian Antarctic expeditions 50 and 51 (Fig. 2a).

We compile velocity-depth functions from sonobuoy/refraction velocity solutions within the areas of the thickest sediments on both margins. We then calculate the average velocity as a function of TWT below the sea floor from these velocity solutions to enable depth conversion of total sediment thickness between the seafloor and basement. Access to refraction data from recent Russian Antarctic expeditions allowed us to extend these velocity solutions to more than 5s TWT below the sea floor. We extrapolate the velocity trends in the deepest sediments to provide velocity functions for depth conversion in the areas where reflection basement is interpreted at greater TWT than the extent of available velocity functions from refraction data.

Given the limited number of velocity solutions available to us, and their uneven spatial distribution, all average velocity-depth functions are co-plotted

regardless of their geographic location. Velocity functions are not averaged across any region, and no differential velocity-depth distribution within a region is taken into account. The high and low velocity boundaries of the resulting corridor of values are approximated by polynomial functions (Figure 2b). Finally, we estimate the maximum and minimum total sediment thicknesses utilizing the maximum and minimum average velocity functions, respectively.

Differences between the minimum and maximum average velocity values reach 1 km/s at 3 sec TWT, and they increase further with depth. This means that total sediment thickness of 3 sec in the time domain may vary from 4 to 6 km in depth with an average value of 5 km. Therefore, sediment thickness variations within ± 1 km between any two locations are within the accuracy of our method.

Differences between the maximum and minimum total sediment thicknesses are due only to difference in velocity functions, not due to ambiguity of basement identification in reflection data, which represents an additional, unquantified source of error.

Gridding and merging

Sediment thickness contours from Géli et al. (2007), covering the region from 60°E to 148°E and 30°S to 60°S, were used for the abyssal plains of the Southeast Indian Ridge. This dataset was pre-processed (using the GMT function `blockmean`) to avoid spatial aliasing and eliminate redundant data. The data were gridded using the GMT function `surface` using a tension factor of 0.7 to suppress local maxima and minima. This tension factor is similar to that used by Smith and Wessel (1990) when gridding regional bathymetric data to match hand-drawn contours. Figure 3a shows the abyssal plain sediment thickness grid

masked at distances further than 20 minutes. The minimum and maximum sediment thickness estimates from seismic reflection and refraction information for the Australian and Antarctic conjugate margins were processed separately using the same approach (Figures 3b and 3c). These data extend across a region from 60°E to 155°E and 30°S to 72°S.

The Australian-Antarctic margin minimum and maximum grids were combined with a masked version of the abyssal plain sediment thickness grid (masked within 2° of the margin data source locations). These combined datasets were then pre-processed and surfaced with a tension factor of 0.7 (Figure 4b and 4c).

Comparisons of the resulting minimum and maximum estimates with each other and the NGDC grid are shown in Figure 5. The maximum sediment thickness estimates for the conjugate Australian and Antarctic margins (Figure 5a) are ~25% thicker than the minimum sediment thickness estimates. This difference is consistent with the velocity-depth profiles used for depth conversion: they diverge by more than 1.0 km/s in the deeper part of the sedimentary section (Figure 2). Both the maximum and minimum sediment thickness estimates for the conjugate margins reveal 1-2 km thicker sediments across large swaths of the margins compared to the NGDC compilation. Sections of both the Antarctic and Australian margins show regions of significantly thicker accumulations, in particular between 100°E-120°E on the Antarctic margin and the Ceduna Plateau on the Australian margin with ~9 km (minimum) to ~13 km more sediment than previously shown.

The sediment thickness grid resulting from combining the minimum sediment thickness estimate for the Australian and Antarctic conjugate margins with Géli

et al.'s (2007) dataset (Figure 4b) over the region 60°E to 155°E and 30°S to 72°S was combined with the global NGDC sediment thickness grid (Divins, 2004).

Blending between our regional grid and the global grid was accomplished using cosine-taper weights across 10° in the longitudinal direction, and 5° in the latitudinal direction (Figure 6b).

Discussion and Conclusion

The NGDC global sediment thickness map for the oceans (Divins, 2004) provides minimum thickness estimates, however extensive collection of seismic reflection and refraction data over the past decade across the conjugate Australian-Antarctic margins have revealed large areas where the actual sediment thickness is much greater than that shown by the global minimum thickness grid. We combine a minimum estimate of these sediment accumulations, computed using velocity-depth functions from co-analysis of the seismic reflection and refraction data, with sediment thickness information from the intervening abyssal plains in order to update the global sediment thickness dataset for the previously poorly represented Southeast Indian Ridge region.

Thick sediments occur on both the conjugate Australian and Wilkes Land margins, however the patterns of sedimentation vary considerably. On the Australian southern margin thick (>4 km) sediment accumulations are present in the Ceduna Sub-basin and the Otway Basin. Large amounts of volcanoclastic sandstones and graywackes were rapidly deposited in the Otway Basin during the Early Cretaceous followed by restricted marine sedimentation of quartz-rich sandstone, marine shale, and fluviodeltaic clastic sequences (Hegarty et al.,

1988). Similarly, significant amounts of the thick sediments in the Ceduna Sub-basin were deposited as prograding, deltaic syn- and post-rift sedimentation during the Cretaceous (Lane et al., 2012; Totterdell and Bradshaw, 2004). In contrast, the thick accumulations of sediment on the Wilkes Land margin are largely due to glacial sedimentation since the Eocene, with only thin syn-rift sequences (Colwell et al., 2006; Lane et al., 2012).

Acknowledgements

Figures in this paper were created using GMT (Wessel and Smith, 1991). S.W. and R.D.M were supported by ARC grant FL0992245. J.W. was supported by Statoil.

References

- Bradshaw, B. E., Rollet, N., Totterdell, J., and Borissova, I., 2003, A revised structural framework for frontier basins on the southern and southwestern Australian continental margin: Geoscience Australia.
- Colwell, J. B., Stagg, H. M. J., Direen, N. G., Bernardel, G., and Borissova, I., 2006, The structure of the continental margin off Wilkes Land and Terre Adélie, East Antarctica, *in* Fütterer, D. K., Damaske, D., Kleinschmidt, G., Miller, H., and Tessensohn, F., eds., *Antarctica: Contributions to Global Earth Sciences*: Berlin, Springer-Verlag, p. 327-340.
- Crosby, A. G., White, N. J., Edwards, G. R. H., Thompson, M., Corfield, R., and Mackay, L., 2011, Evolution of deep-water rifted margins: Testing depth-dependent extensional models: *Tectonics*, v. 30, p. TC1004, doi:10.1029/2010TC002687.

Divins, D. L., 2004, Total sediment thickness of the world's oceans and marginal seas, National Geophysical Data Center.

GEBCO, 2008, The GEBCO_08 Grid, version 20100927, <http://www.gebco.net>.

Géli, L., Cochran, J., Lee, T., Francheteau, J., Labails, C., Fouchet, C., and Christie, D., 2007, Thermal regime of the Southeast Indian Ridge between 88°E and 140°E: Remarks on the subsidence of the ridge flanks: *J. Geophys. Res.*, v. 112, no. B10, p. B10101.

Hegarty, K. A., Weissel, J. K., and Mutter, J. C., 1988, Subsidence history of Australia's southern margin: constraints on basin models: *American Association of Petroleum Geologists Bulletin*, v. 74, p. 615-633.

Lane, H., Müller, R. D., Totterdell, J. M., and Whittaker, J., 2012, Developing a consistent sequence stratigraphy for the Wilkes Land and Great Australian Bight margins, *Eastern Australasian Basins Symposium IV*: Brisbane, Queensland.

Sayers, J., Symonds, P. A., Direen, N. G., and Bernadel, G., 2001, Nature of the continent-ocean transition on the non-volcanic rifted margin in the central Great Australian Bight, *in* Wilson, R. C. L., Whitmarsh, R. B., Taylor, B., and Froitzheim, N., eds., *Non-volcanic rifting of continental margins: a comparison of evidence from land and sea*, Volume Special Publication, Geological Society of London, p. 51-76.

Seton, M., Müller, R., Zahirovic, S., Gaina, C., Torsvik, T., Shephard, G., Talsma, A., Gurnis, M., Turner, M., and Chandler, M., 2012, Global continental and ocean basin reconstructions since 200 Ma: *Earth-Science Reviews*.

Smith, W. H. F. a. P. W., 1990, Gridding with continuous curvature splines in tension: *Geophysics*, v. 55, p. 293–305.

Stagg, H. M. J., Colwell, J. B., Direen, N. G., O'Brien, P. E., Browning, B. J., Bernardel, G., Borissova, I., Carson, L., and Close, D. I., 2005, Geological framework of the continental margin in the region of the Australian Antarctic Territory: Geoscience Australia Record, 2004/25.

Totterdell, J. M., and Bradshaw, B. E., 2004, The structural framework and tectonic evolution of the Bight Basin, PESA Eastern Australasian Basins Symposium II: Adelaide, Australia, PESA.

Wessel, P., and Smith, W. H. F., 1991, Free software helps map and display data: EOS Trans. AGU, v. 72, p. 445-446.

Whittaker, J. M., Müller, R. D., and Gurnis, M., 2010, Development of the Australian-Antarctic depth anomaly: *Geochemistry Geophysics Geosystems*, v. 11, no. 11, p. Q11006.

Figure 1: Regional bathymetric map (GEBCO, 2008) showing locations of velocity data from seismic refraction and sonobuoy sources (black dots), and seismic reflection profile locations (red lines) along the Australian and Antarctic margins. Continent-ocean boundary (blue line) from Seton et al. (2012).

Figure 2. a) Example of refraction seismic data recorded by a sonobuoy on one of the lines of the Russian Antarctic expedition 50, offshore Wilkes Land.

Apparent seismic velocity values (km/s) are annotated next to the first arrivals. Phases of 3.5 and 4.3 km/s velocities are from the sedimentary section; 5.4 and 6.7 km/s – from the upper and lower parts of the oceanic crust respectively; 8.0 km/s – from the upper mantle. b) Minimum and maximum average seismic

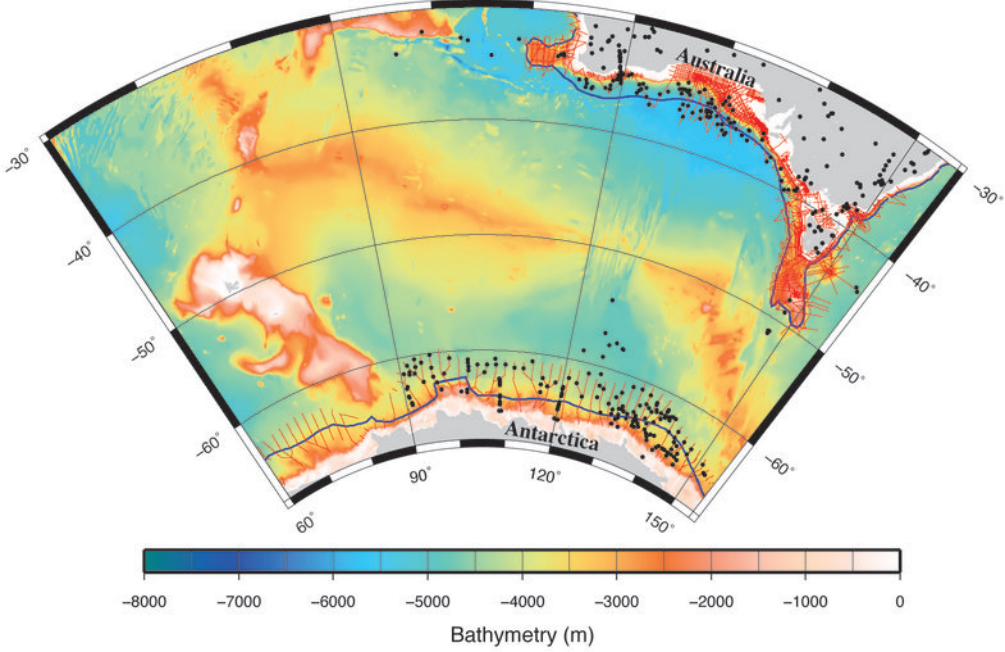
velocity trends from refraction seismic interpretation used for depth conversion of total sediment thickness

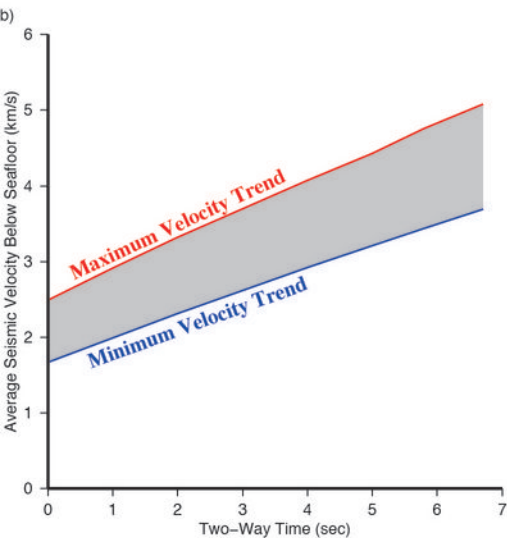
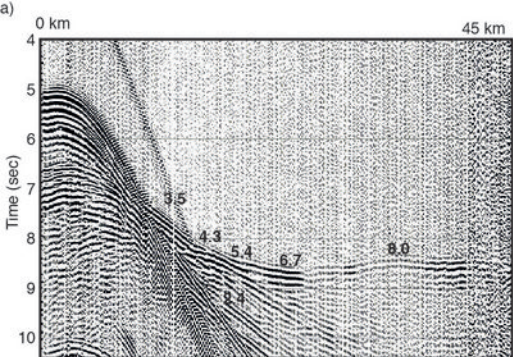
Figure 3: a) Sediment thickness estimates from Géli et al. (2007), b) computed minimum sediment thickness estimates for the Australian southern margin and Antarctic Wilkes Land margin, and c) computed max sediment thickness estimates sediment thickness for the Australian southern margin and Antarctic Wilkes Land margin. Black line is the continent-ocean boundary from Seton et al. (2012).

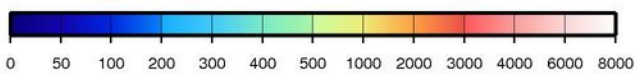
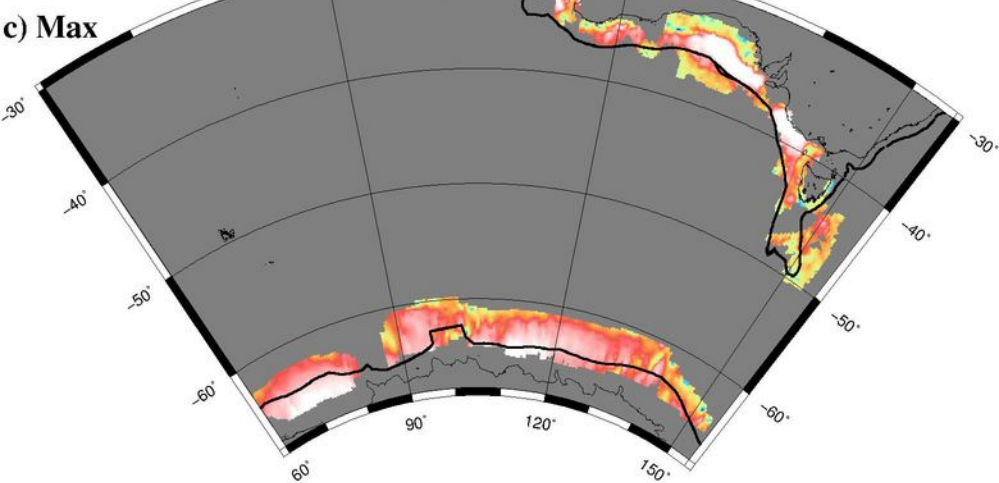
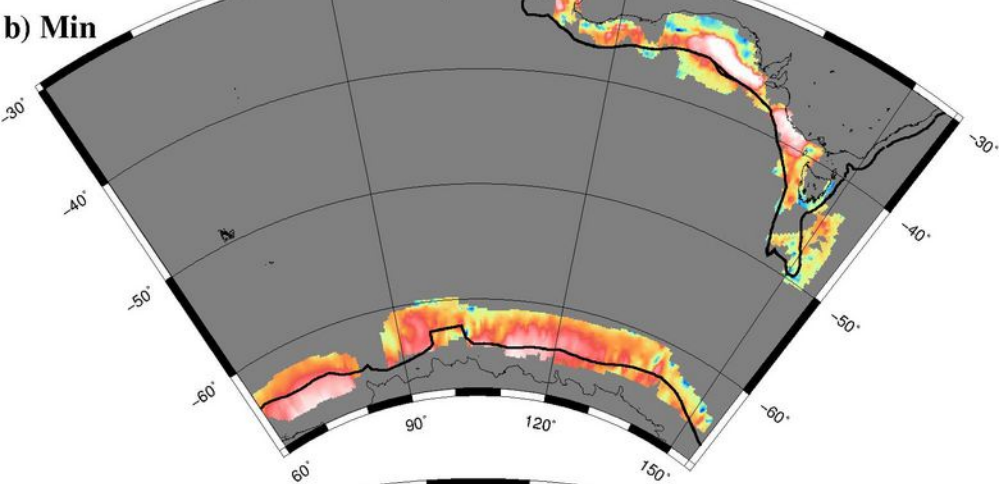
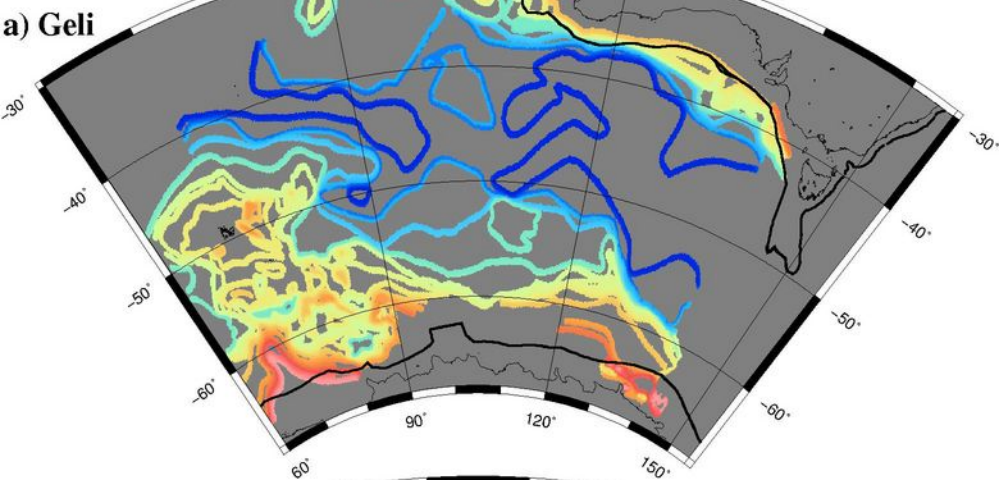
Figure 4: a) NGDC sediment thickness grid (Divins, 2004). Revised sediment thicknesses using the refraction-derived b) minimum, and c) maximum estimates for the Australian and Antarctic extended margins combined with sediment thickness data for the abyssal plains from Géli et al. (2007). Black line is the continent-ocean boundary from Seton et al. (2012).

Figure 5: a) Difference between the minimum and maximum sediment thickness estimates from this paper, b) Difference between the minimum estimate and the NGDC estimate, and c) Difference between the maximum estimate and the NGDC estimate. Black line is the continent-ocean boundary from Seton et al. (2012).

Figure 6: Regional comparison of a) the 5-minute NGDC minimum sediment thickness grid (Divins, 2004), with b) our updated 5-minute minimum sediment thickness grid.

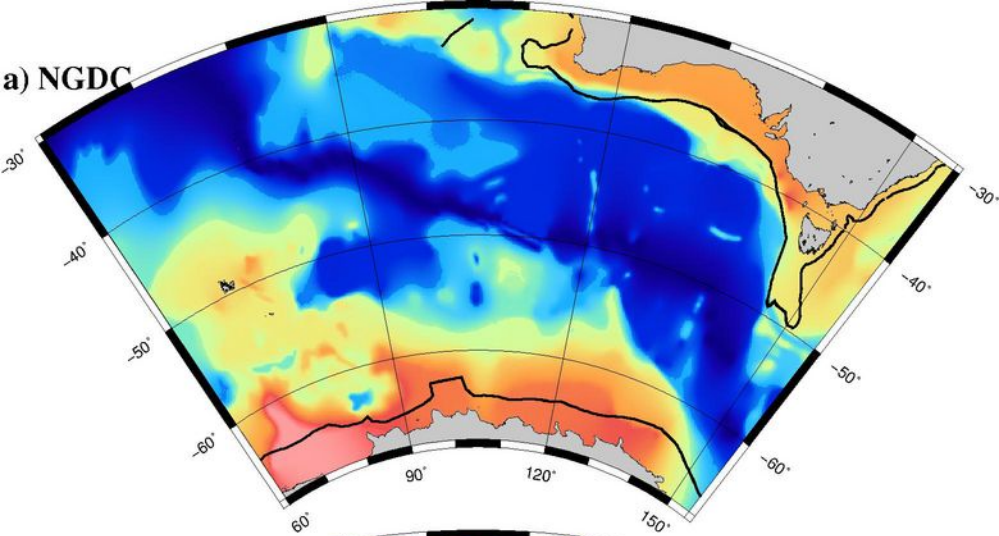




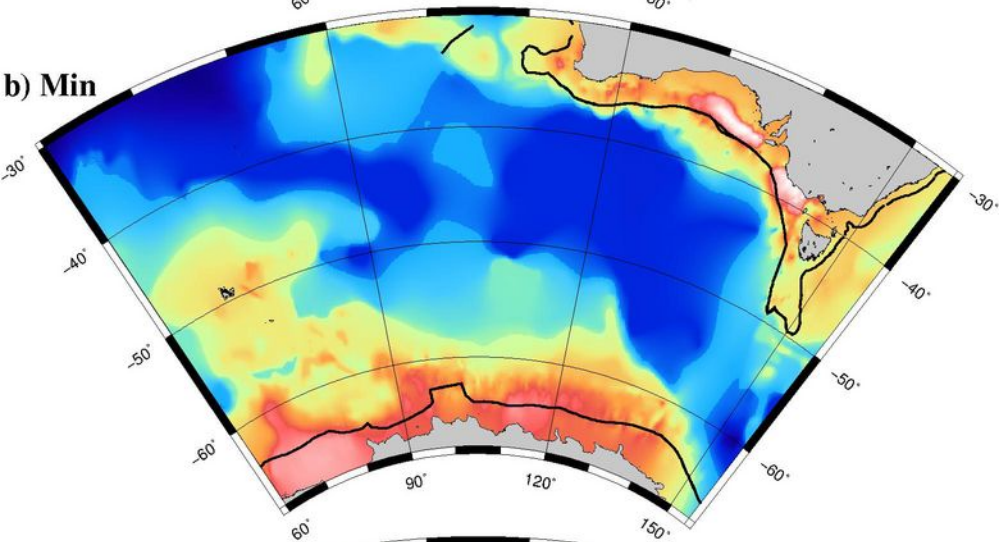


Sediment Thickness [m]

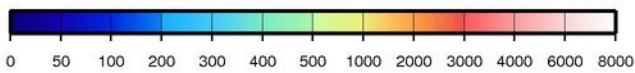
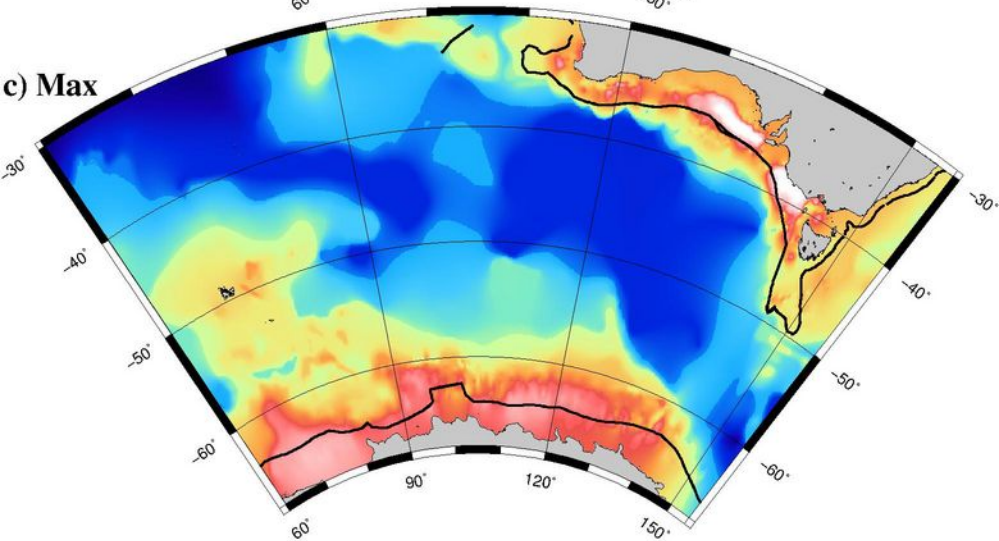
a) NGDC



b) Min

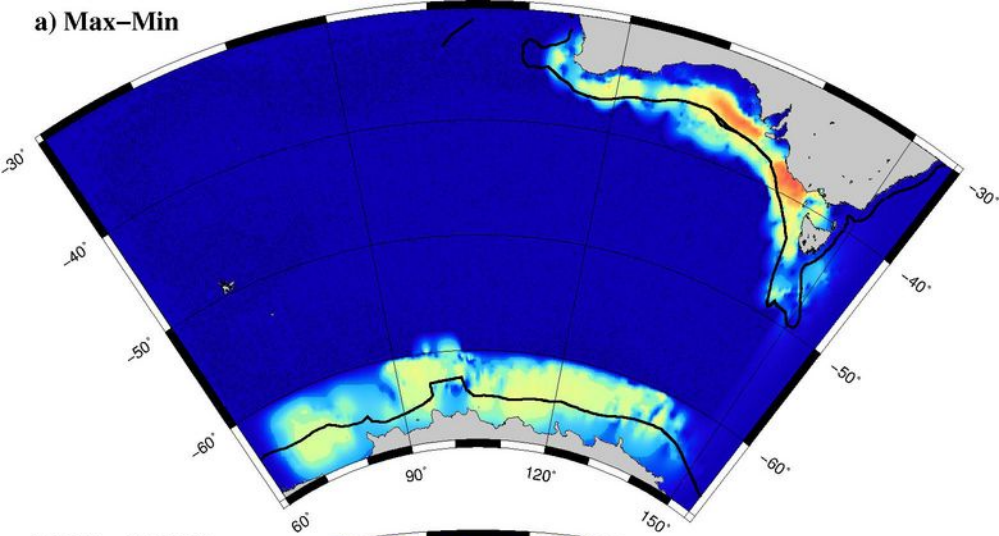


c) Max

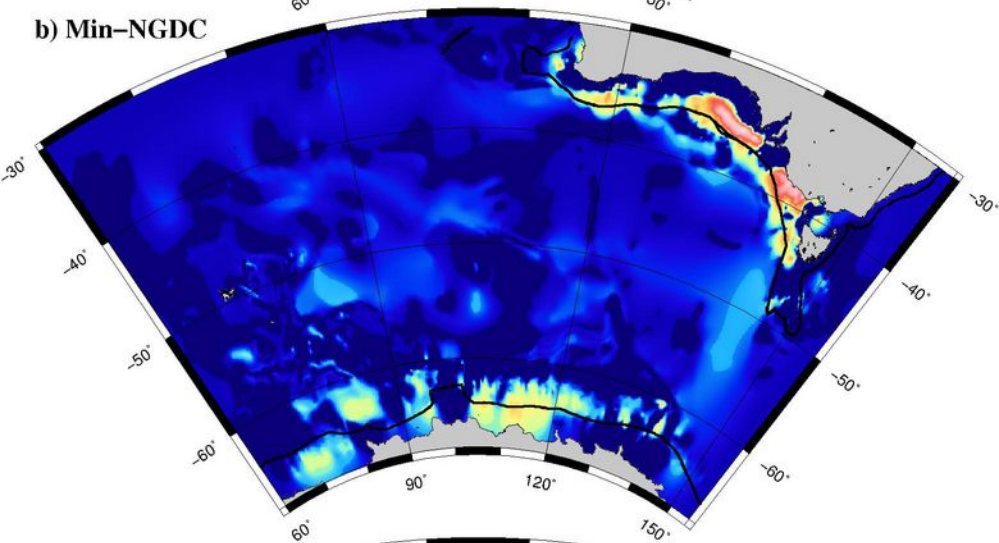


Sediment Thickness [m]

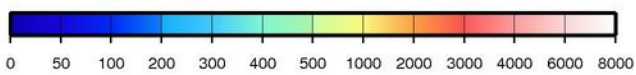
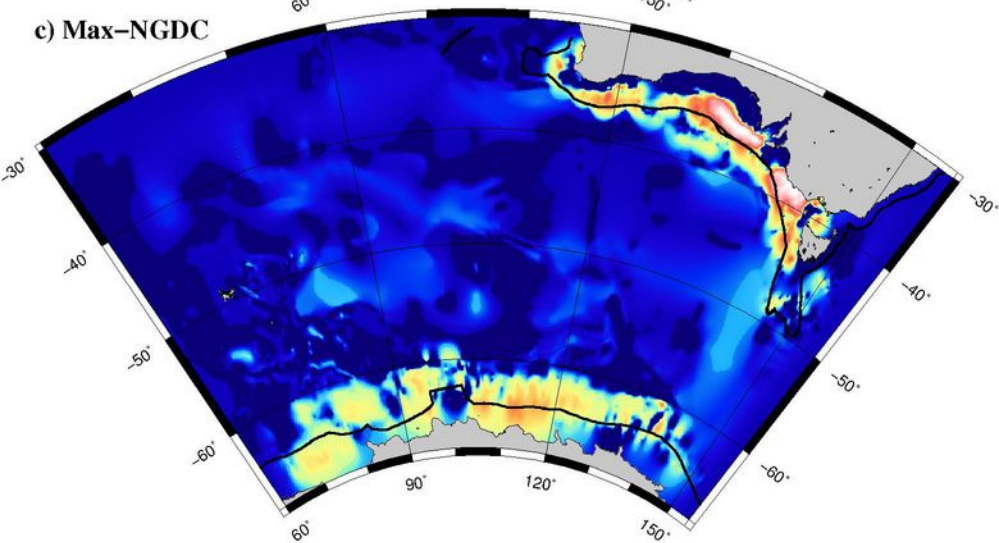
a) Max-Min



b) Min-NGDC

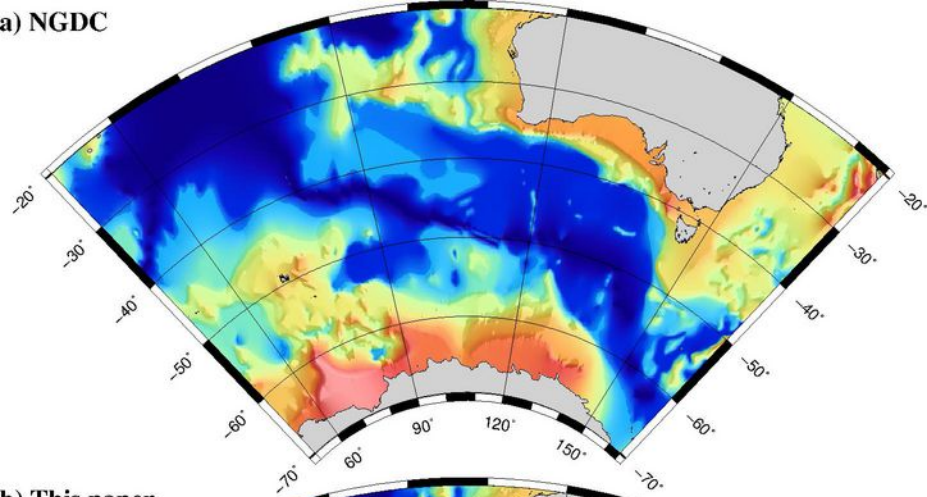


c) Max-NGDC

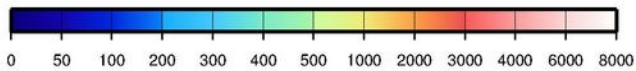
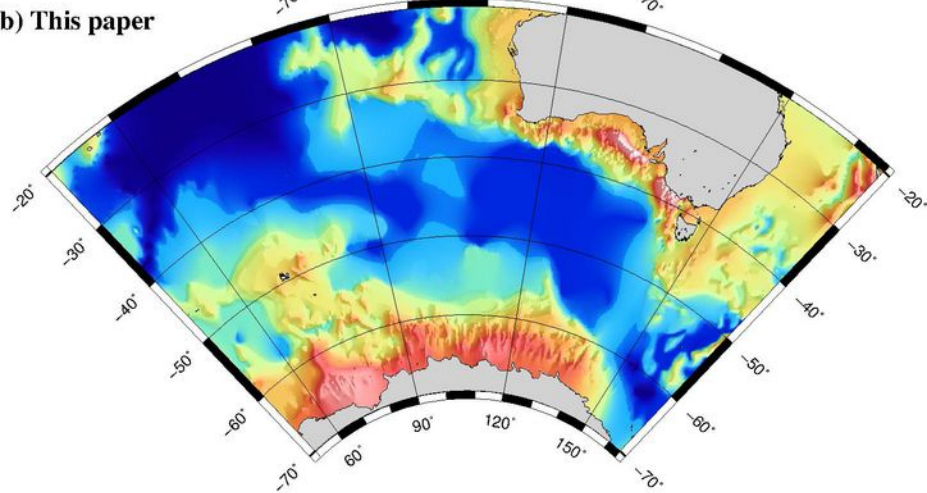


Sediment Thickness [m]

a) NGDC



b) This paper



Sediment Thickness [m]